A Decentralized Cooperative Control Scheme With Obstacle Avoidance for a Team of Mobile Robots

Hamed Rezaee, *Student Member, IEEE*, and Farzaneh Abdollahi, *Member, IEEE*

***Abstract*—The problem of formation control of a team of mobile robots based on the virtual and behavioral structures is considered in this paper. In the virtual structure, each mobile robot is modeled by an electric charge. The mobile robots move toward a circle, and due to repulsive forces between the identical charges, regular polygon formations of the mobile robots will be realized. For swarm formation, a virtual mobile robot is located at the center of the circle, and other mobile robots follow it. In the introduced approach, each mobile robot finds its position in the formation autonomously, and the formation can change automatically in the case of change in the number of the mobile robots. This paper also proposes a technique for avoiding obstacles based on the behavioral structure. In this technique, when a mobile robot gets close to an obstacle, while moving toward its target, a rotational potential field is applied to lead the mobile robot to avoid the obstacle, without locating in local minimum positions.**

***Index Terms*—Cooperative control, local minima, mobile robots, multiagent systems, obstacle avoidance.**

I. Introduction

THE FORMATION control of multiagent systems has received many researchers' attention in recent years. This attention is due to its applications in several fields such as mobile robots, unmanned surface vessels, autonomous underwater vehicles, and unmanned aerial vehicles. Among these vehicles, mobile robots have found many applications for exploration, surveillance, search and rescue missions, agriculture, and so on [1]–[5].

Three main structures are considered for the formation control of multiagent systems in the literature, namely: leader–follower, virtual, and behavioral structures, each of whom has its own advantages and disadvantages. In the leader–follower structure, one agent is considered as a leader, and the other agents are followers which track the leader. In this structure, since only the followers track the leader and there is no feedback from the followers to the leader, if a follower fails to follow properly, no mechanism can guarantee the formation keeping. However, this structure is easy to implement and understand. In the virtual structure, all the agents have a rigid geometric relationship based on a virtual point or virtual leader to provide polygon formations [6]. A merit of this structure is that the virtual leader never fails, and the rigid formation will be maintained during the swarming. This structure, however, cannot reconfigure the formation. In the behavioral structure, while seeking a target, collision or obstacle avoidance are important issues, and the desired behaviors are prescribed for each agent accordingly (see [7], [8], and references therein).

In the view of communication networks, two approaches have been introduced for the formation control of multiagent systems in the literature, namely, centralized and decentralized approaches. In the centralized approach, the control of each agent is based on control signals received from a central controller. The central controller receives the states of all the agents; then, considering all the agents as a system, control signals are provided by the central controller. The advantage of this method is that, in emergency conditions, a human operator can override the control. However, it is not robust in the presence of disturbances and faults in the central controller, whereas in the decentralized approach, each agent makes a decision based on the information of other agents achieved via its own sensors. Therefore, each agent provides its own control input without considering dynamics and control inputs of other agents [9], [10].

The repulsive force method has been employed for swarming and collision and obstacle avoidance of multiagent systems in the literature [11]–[13]. In this paper, it is proposed to apply this method in the formation control of multiagent systems based on the virtual structure. This paper addresses a technique for decentralized virtual structural based formation control of mobile robots. Since all regular polygon formations can be considered on a circle, the mobile robots are located on a circle with a predefined radius around a virtual point which is the center of the circle. Then, to achieve regular polygon formations such as triangles, squares, pentagons, and so on, each mobile robot is modeled by an electric charge which repulses other charges. If the electric charges are identical and the mobile robots are structurally similar, mobile robots reach a stable formation with equal distances from their neighbors. By considering a virtual mobile robot at the center of the formation, the swarming of the formation is realized, and the geometric relationship between the mobile robots is maintained during maneuvers. Although most approaches used the virtual structure which cannot change the configuration of the formation [6], [14], [15], in the proposed approach in this paper, each mobile robot finds its position in the formation autonomously on a regular polygon. In this condition, the formation can change to another regular polygon formation when the number of the

Manuscript received August 14, 2011; revised October 9, 2012 and December 8, 2012; accepted January 17, 2013. Date of publication February 6, 2013; date of current version July 18, 2013.

H. Rezaee is with the Department of Electrical Engineering, Amirkabir University of Technology (Tehran Polytechnic), Tehran 15914, Iran (e-mail: h.rezaee@aut.ac.ir).

F. Abdollahi is with the Department of Electrical Engineering, Amirkabir University of Technology (Tehran Polytechnic), Tehran 15914, Iran, and also with Concordia University, Montreal, QC H3G 1M8, Canada (e-mail: f_abdollahi@aut.ac.ir).

Color versions of one or more of the figures in this paper are available online at http://ieeexplore.ieee.org.

Digital Object Identifier 10.1109/TIE.2013.2245612

agents changes. It can be useful when one of the mobile robots fails or exits or a new mobile robot enters the formation.

An important problem in the swarming of multiagent systems is maintaining the cohesion and stability when agents avoid obstacles. Several techniques such as neural network, fuzzy control, and so on were introduced to address the obstacle avoidance and path planning of autonomous agents [16]–[18]. Using potential fields and repulsive forces exerted by obstacles also is a popular technique that was employed in several approaches. In [11], the center of the gravity of the local swarm attracted the mobile robots, and the stability of the swarm was guaranteed. In that paper, repulsive forces were applied for each mobile robot to avoid collision with obstacles and other mobile robots. In [12], each obstacle was enclosed in a convex polygon, and they produced repulsive forces to avoid collision. In [19], repulsive forces produced by obstacles were used for obstacle avoidance. In [20], a potential field was employed to avoid the collision of unmanned helicopters with obstacles. When an unmanned helicopter approached an obstacle, the repulsive potential field increased and led it far from the obstacle. A similar approach was applied in [21] for obstacle avoidance of autonomous underwater vehicles. In these mentioned papers, however, if a vehicle moves in the opposite direction of the potential field, it may not be able to pass the obstacle, and it may stick in a local minimum position since the resultant vector of the vehicle motion and the repulsive vector from the obstacle may be zero. In the proposed approach in this paper, the potential field produces rotational repulsive vectors. Therefore, in the introduced rotational potential field, directions of the vectors are adjusted to the direction of an approaching mobile robot to lead it toward its target without locating in local minimum positions. This technique can be applied for obstacle avoidance of a swarm formation which is based on the virtual or leader–follower structure. The preliminary versions of the proposed approaches have been presented in [8] and [22] with less details and elaborations.

The remainder of this paper is organized as follows. In Section II, the dynamics of the mobile robots are defined. Section III proposes the approach for swarm formation of mobile robots based on the virtual structure. Section IV presents our approach for obstacle avoidance of mobile robots based on the behavioral structure. Simulation results are given in Section V, and Section VI concludes this paper.

II. Agent Model Definition

Consider a multiagent system containing N fully actuated mobile robots without motion constraints. The dynamical equations of the kth mobile robot are considered as follows:

$$M\ddot{x}_k + B\dot{x}_k = f_{xk} - k_d\dot{x}_k,$$
$$M\ddot{y}_k + B\dot{y}_k = f_{yk} - k_d\dot{y}_k \tag{1}$$

where (x_k, y_k) is the coordinate of the mobile robot, M is the mass, B is the damper coefficient, $f_k = (f_{xk}, f_{yk})$ is the control force, and k_d is a coefficient considered to control the transient response of the mobile robot. In other words, a large value of k_d decreases the overshoot in the system but decreases the speed of the mobile robot. It should be noted that the mentioned parameters and variables are considered nondimensional.

In the next section, a control strategy to lead the mobile robots toward a circle for formation control is presented.

III. Regular Polygon Formation Based on the Virtual Structure

In this section, a method for formation control of mobile robots based on the virtual structure is addressed. At first, (f_{xk}, f_{yk}) in (1) is defined to enforce the kth mobile robot to move toward a circle with radius α and center (x_c, y_c). Then, a control strategy for regular polygon formations of mobile robots on the circle will be presented.

A. Mobile Robot Motion Control

Lemma 1 introduces the desired trajectory which attracts the mobile robots toward a circle.

Lemma 1: Equation (2) provides a trajectory toward a circle with center (x_c, y_c) and radius α such that, when the states get to the circle, they will stop moving

$$\dot{x} = -(x - x_c)\left((x - x_c)^2 + (y - y_c)^2 - \alpha^2\right),$$
$$\dot{y} = -(y - y_c)\left((x - x_c)^2 + (y - y_c)^2 - \alpha^2\right) \tag{2}$$

where $(x, y) \neq (x_c, y_c)$.

Proof: By employing the polar coordinate $r^2 = (x - x_c)^2 + (y - y_c)^2$ and $\theta = \arctan((y - y_c)/(x - x_c))$ to (2), the following equations can be achieved:

$$\dot{r} = -r(r^2 - \alpha^2) \quad \dot{\theta} = 0. \tag{3}$$

The main target is to converge to a circle with center (x_c, y_c) and radius α, i.e., $r = \alpha$. Therefore, we should show that r converges to α and $\dot{r}$ converges to zero. Let us define an error $e = r - \alpha$ and a Lyapunov function $V(e) = e^2$; therefore,

$$\dot{V}(e) = 2e\dot{r}. \tag{4}$$

Substituting $\dot{r}$ from (3) into (4) yields $\dot{V}(e) = -2e^2r(r + \alpha)$. From $(x, y) \neq (x_c, y_c)$, it can be said that $r > 0$. Since $r > 0$ and $\alpha > 0$, one can get $\dot{V}(e) \leq 0$. Therefore, e and also r are bounded, and $\dot{V}(e)$ converges to zero. On the other hand, the only solution of $V(e) = 0$ is $e = 0$. In other words, all trajectories converge to the circle, and since $\dot{\theta} = 0$, when the states move toward the circle, they do not have rotational motion, and this proves the lemma. ■

Lemma 1 provides us a guideline to find the proper direction of the mobile robot in (1), i.e., by considering the result of Lemma 1, input force (f_{xk}, f_{yk}) in (1) is defined as follows:

$$f_{xk} = -k_{sk}\left((x_k - x_c)\left((x_k - x_c)^2 + (y_k - y_c)^2 - \alpha^2\right)\right)$$
$$f_{yk} = -k_{sk}\left((y_k - y_c)\left((x_k - x_c)^2 + (y_k - y_c)^2 - \alpha^2\right)\right) \tag{5}$$

where k_{sk} is a positive gain.

The next section extends the proposed control strategy for regular polygon formations of mobile robots on the circle.

B. Mobile Robot Formation

We target to arrange the mobile robots in a regular polygon formation. To achieve this goal, each mobile robot is modeled by an electric charge. If all the charges are negative or positive, they repulse each other. Let us consider all the mobile robots with identical charges and define a virtual point at (x_c, y_c). The force defined in (5) holds the mobile robots on a circle with radius α and center (x_c, y_c), and they cannot move far while they repulse each other. In other words, when the force defined in (5) is larger than the resultant of the repulsive forces in the direction of the radius of the circle, it can keep the mobile robots on the circle. Since the electric charges are identical, they reach equilibrium points if the distances between them are identical. Because, in this condition, the resultant of the repulsive forces tangent to the circle is zero, therefore, a regular polygon formation of the mobile robots on the circle can be obtained. The repulsive force between each two electric charges is defined as follows:

$$F_{ki} = k_r \frac{q_k q_i}{r_{ki}^2}$$

where F_{ki} is the force between the kth and ith electric charges, k_r is a positive constant coefficient, q_i and q_k are the electric charges, and r_{ki} is the distance between the two electric charges. Therefore, the force that exerts on the kth charge from $N-1$ charges is as follows:

$$F_k = k_r q_k \sum_{i=1, i\neq k}^{N} \frac{q_i}{r_{ki}^2} \tag{6}$$

where it can be decomposed on the x- and y-axes as follows:

$$F_{xk} = k_r \sum_{i=1, i\neq k}^{N} \frac{q_k q_i}{r_{ki}^2} \cos(\theta_{ki}),$$
$$F_{yk} = k_r \sum_{i=1, i\neq k}^{N} \frac{q_k q_i}{r_{ki}^2} \sin(\theta_{ki})$$

where

$$\cos(\theta_{ki}) = \frac{x_k - x_i}{|r_{ki}|} \quad \sin(\theta_{ki}) = \frac{y_k - y_i}{|r_{ki}|}.$$

Hence, the dynamics of the kth mobile robot in the proposed virtual structure can be stated as follows:

$$M\ddot{x}_k + B\dot{x}_k = f_{xk(\mathrm{VS})} - k_d \dot{x}_k,$$
$$M\ddot{y}_k + B\dot{y}_k = f_{yk(\mathrm{VS})} - k_d \dot{y}_k \tag{7}$$

where

$$f_{xk(\mathrm{VS})} = F_{xk} - k_{sk} \times \left((x_k - x_c)\left((x_k - x_c)^2 + (y_k - y_c)^2 - \alpha^2\right)\right),$$
$$f_{yk(\mathrm{VS})} = F_{yk} - k_{sk} \times \left((y_k - y_c)\left((x_k - x_c)^2 + (y_k - y_c)^2 - \alpha^2\right)\right). \tag{8}$$

It should be noted that, in (6), the repulsive force is proportional to $1/r_{ki}^2$. This states that each agent will be repulsed by near agents or neighboring agents. The following example illustrates the mentioned formation strategy.

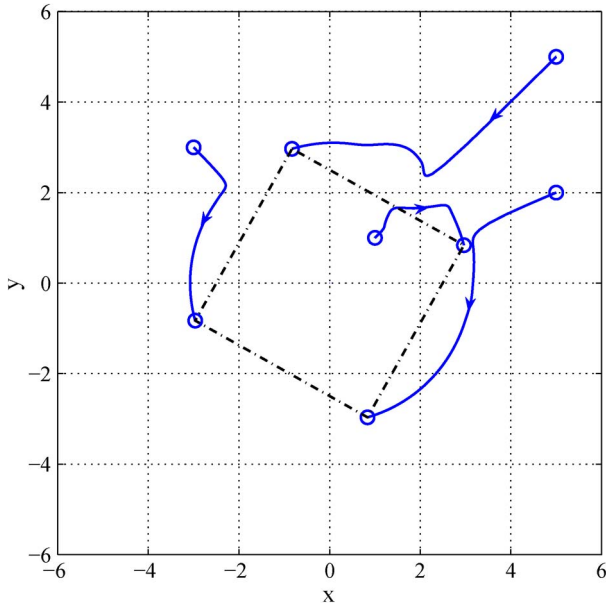

Fig. 1. Regular polygon formation in Example 1.

Example 1: Consider four mobile robots with initial positions $(-3, 3)$, $(1, 1)$, $(5, 2)$, and $(5, 5)$ and dynamical equations defined in (7) and (8), where $M = 1$, $B = 1$, $k_d = 9$, $k_{sk} = 1$, $k_r = 0.15$, $(x_c, y_c) = (0, 0)$, $\alpha = 3$, and $q_k = 10$, $k \in \{1, 2, 3, 4\}$. The square formation of the four mobile robots is depicted in Fig. 1.

An advantage of the proposed method is that each mobile robot finds its equilibrium point and proper position to locate in the regular polygon formation autonomously, and it is not necessary to set the position of each mobile robot in the formation. This equilibrium point depends on the initial position of the mobile robot which means that, if we change the label of the agents, the provided formation and the positions of the agents in the formation do not change. Therefore, since the equilibrium points of the agents are on regular polygon formations, the proposed approach is useful when the number of the agents changes during maneuvers due to the mobile robot failures or adding new ones to the system. In other words, a change in the number of the agents leads to reach another regular polygon formation.

It should be noted that the mobile robots move toward the circle and each mobile robot is repulsed from other mobile robots. In Fig. 2, the attractive force toward the circle is shown by f_k defined in (5), the repulsive force resultant from other agents is shown by F_k defined in (6), and it is decomposed into two terms: F_k' perpendicular to the circle radius (tangent to the circle) and F_k'' in the direction of the circle radius. To keep the kth mobile robot on the circle, the resultant of the repulsive forces exerted on it should be smaller than the attractive force toward the circle; in other words, f_k should be larger than F_k''. It means that k_{sk} in (5) should be chosen large relative to $k_r q_k q_i$ $(q_k = q_i)$ in (6) to hold the mobile robots on the circle with favorite errors.

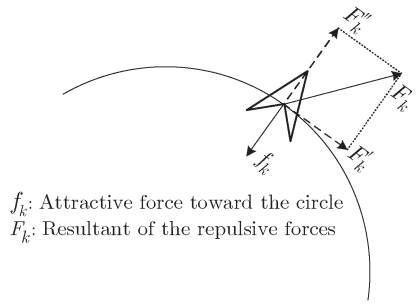

Fig. 2. Forces exerted on the kth mobile robot.

In this condition, the equilibrium positions of N agents are on the vertices of a regular polygon formation (with N sides or N vertices). Because, in a regular polygon formation, the sides are identical, the resultant of the repulsive forces exerted on each agent tangent to the circle is zero, i.e., $F'_k = 0$, $k \in \{1, 2, \ldots, N\}$.

C. Swarm Formation for the Virtual Structure

In the previous section, the mobile robots were positioned in a regular polygon formation around a circle with radius α and center (x_c, y_c). For swarm formation control of the mobile robots, a virtual mobile robot should be considered at the center of the circle that tracks a trajectory. The mobile robots placed on the circle adjust themselves to the virtual leader and therefore follow its trajectory. Therefore, the force $(f_{xk(\mathrm{VS})}, f_{yk(\mathrm{VS})})$ for the kth mobile robot in (8) is modified as follows:

$$\begin{aligned} f_{xk(\mathrm{VS})} =& F_{xk} - k_{sk} \\ & \times \left((x_k - x_v)\left((x_k - x_v)^2 + (y_k - y_v)^2 - \alpha^2\right)\right), \\ f_{yk(\mathrm{VS})} =& F_{yk} - k_{sk} \\ & \times \left((y_k - y_v)\left((x_k - x_v)^2 + (y_k - y_v)^2 - \alpha^2\right)\right) \end{aligned} \quad (9)$$

where (x_v, y_v) is the coordinate of the virtual mobile robot. The dynamics of the virtual mobile robot can be expressed as follows:

$$\begin{aligned} M\ddot{x}_v + B\dot{x}_v &= f_{xv} - k_d\dot{x}_v, \\ M\ddot{y}_v + B\dot{y}_v &= f_{yv} - k_d\dot{y}_v \end{aligned} \quad (10)$$

where (f_{xv}, f_{yv}) is a virtual force.

The obtained regular polygon formation is based on the repulsive effect of the mobile robots; therefore, it is not necessary to control the distance between the mobile robots directly. The problem of the virtual structure is the formation changing during maneuvers, while the proposed approach in this paper can change the formation automatically when some mobile robots exit or enter the formation.

IV. Obstacle Avoidance in the Behavioral Structure

In this section, at first, a control scheme for obstacle avoidance of mobile robots is proposed. Then, it will be extended for a team of mobile robots based on the behavioral structure.

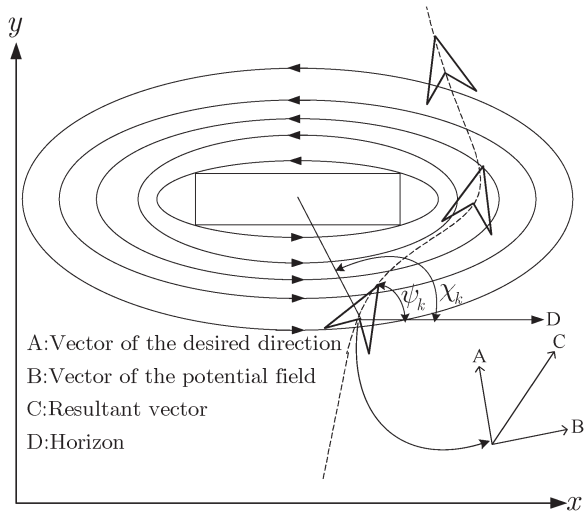

Fig. 3. Potential field around an obstacle and the trajectory of an approaching mobile robot.

A. Obstacle Avoidance

This section proposes a technique for obstacle avoidance of mobile robots based on a rotational potential field. The main advantage of the proposed obstacle avoidance technique is that the repulsive forces from an obstacle are adaptive with the motion of the mobile robot. In other words, the potential field vectors rotate around the obstacle whose directions depend on the motion direction of the mobile robot.

For instance, as depicted in Fig. 3, in a case that a mobile robot is approaching an obstacle in its left-hand side, the rotational potential field around the obstacle is counterclockwise. The direction of the potential field can be clockwise when the mobile robot approaches in the opposite direction. Therefore, the potential field will not be in the opposite direction of the approaching mobile robot, and the resultant input force on the mobile robot will not be zero. Therefore, the mobile robot will not stick in a local minimum position.

Without loss of generality, an obstacle is considered as a rectangle in the direction of the x- and y-axes whose center and dimension will be identified via the mobile robot sensors. As shown in Fig. 3, an ellipse is considered around the obstacle whose equation is proportional to the location and dimension of the obstacle. This ellipse has minimum area that passes through the vertices of the rectangle, and the defined rotational potential field vectors are on ellipses parallel to this ellipse. The following lemma provides the equation of the ellipse with minimum area.

Lemma 2: The equation of an ellipse with minimum area which envelopes a rectangle with $(x_o \pm v_1, y_o \pm v_2)$ as its vertices is given as follows:

$$\frac{1}{2v_1^2}(x - x_o)^2 + \frac{1}{2v_2^2}(y - y_o)^2 = 1 \quad (11)$$

where (x_o, y_o) is the center of the rectangle.

Proof: Consider an ellipse with

$$A^2(x - x_o)^2 + B^2(y - y_o)^2 = 1. \quad (12)$$

The area of the ellipse is proportional to $1/AB$. Therefore, to achieve the minimum area of the ellipse, AB and also $(AB)^2$ should be maximum. By substituting the coordinates of the rectangle vertices in (12), it can be stated that

$$A^2v_1^2 + B^2v_2^2 = 1 \Rightarrow B^2 = \frac{1 - A^2v_1^2}{v_2^2}. \tag{13}$$

Therefore, the maximum $(AB)^2$ can be obtained by the following conditions:

$$\frac{\partial (AB)^2}{\partial A} = 0. \tag{14}$$

By substituting (13) in (14), since $A \neq 0$, one can get $A^2 = 1/2v_1^2$, and then, $B^2 = 1/2v_2^2$. Therefore, by substituting A^2 and B^2 in (12), (11) is achieved, and this proves the lemma. ■

Therefore, the equation of an ellipse with minimum area around an obstacle on the $x - y$ plane whose vertices are $(x_o \pm v_1, y_o \pm v_2)$ can be stated as follows:

$$A^2(x - x_o)^2 + B^2(y - y_o)^2 = 1$$

where $A^2 = 1/2v_1^2$ and $B^2 = 1/2v_2^2$. The potential field vectors are parallel to this ellipse, on ellipses which can be expressed by the following equation:

$$\hat{A}^2(x - x_o)^2 + \hat{B}^2(y - y_o)^2 = 1 \tag{15}$$

where $\hat{A}/\hat{B} = A/B$. On the other hand, the potential field is rotational on these ellipses. Lemma 3 provides required state space equations with trajectories rotating around the introduced ellipses in (15).

Lemma 3: In the following state space equations, the trajectories of the states with any initial positions rotate on the ellipses $\hat{A}^2(x - x_o)^2 + \hat{B}^2(y - y_o)^2 = 1$ in the clockwise direction:

$$\dot{x} = \frac{\hat{B}}{\hat{A}}(y - y_o),$$
$$\dot{y} = -\frac{\hat{A}}{\hat{B}}(x - x_o). \tag{16}$$

Proof: By defining the polar coordinate $r^2 = \hat{A}^2(x - x_o)^2 + \hat{B}^2(y - y_o)^2$ and $\theta = \arctan((y - y_o)/(x - x_o))$ and substituting them in (16), one can get $\dot{r} = 0$ and $\dot{\theta} = -1$, and this proves the lemma. ■

It should be noted that the clockwise direction of the vectors in (16) can be reversed by inverting the sign of $\dot{x}$ and $\dot{y}$. To avoid a sudden change in the direction of the mobile robot approaching the obstacle and to avoid locating in local minimum positions, the direction of the potential field is determined based on the direction of the kth approaching mobile robot, i.e., $\psi_k = \arctan 2(\dot{y}_k, \dot{x}_k)$ (when it gets close to the potential field vectors). The direction ψ_k should be compared with the angle between the line linking the mobile robot and the center of gravity of the obstacle and the horizontal axis which is indicated by χ_k. Therefore, based on the aforementioned reasons, in a case that the mobile robot approaches the obstacle with $\psi_k \geq \chi_k$, it is proper to move in the clockwise direction. In the other case that $\psi_k < \chi_k$, the vector direction should be counterclockwise. The angle between the line linking the mobile robot and the center of gravity of the obstacle and the horizontal axis can be obtained as follows:

$$\chi_k = \arctan 2(y_o - y_k, x_o - x_k)$$

where χ_k and ψ_k are shown in Fig. 3. Since $-\pi \leq \arctan 2(.) \leq \pi$, therefore, $-\pi \leq \chi_k \leq \pi$, and $-\pi \leq \psi_k \leq \pi$. On the other hand, in the proposed approach, ψ_k and χ_k are considered between 0 and 2π; therefore, they can be compared as follows:

$$\psi_k \geq \chi_k \quad \text{if} \quad \text{mod}(\psi_k - \chi_k, 2\pi) \leq \pi,$$
$$\psi_k < \chi_k \quad \text{if} \quad \text{mod}(\psi_k - \chi_k, 2\pi) > \pi$$

where mod(.) is the modulus after division.

Considering the aforementioned issues, the rotational vectors around the obstacle can be stated as follows:

$$f_{kr} = f_{xkr}i + f_{ykr}j \tag{17}$$

where

$$f_{xkr} = f_{xkrc}, f_{ykr} = f_{ykrc} \qquad \psi_k \geq \chi_k$$
$$f_{xkr} = f_{xkrcc}, f_{ykr} = f_{ykrcc} \qquad \psi_k < \chi_k$$

and (f_{xkrc}, f_{ykrc}) and (f_{xkrcc}, f_{ykrcc}) respectively show the clockwise and counterclockwise force vectors as follows:

$$f_{xkrc} = \frac{\hat{B}}{\hat{A}}(y_k - y_o) = \frac{B}{A}(y_k - y_o)$$
$$f_{ykrc} = -\frac{\hat{A}}{\hat{B}}(x_k - x_o) = -\frac{A}{B}(x_k - x_o) \tag{18}$$
$$f_{xkrcc} = -\frac{\hat{B}}{\hat{A}}(y_k - y_o) = -\frac{B}{A}(y_k - y_o)$$
$$f_{ykrcc} = \frac{\hat{A}}{\hat{B}}(x_k - x_o) = \frac{A}{B}(x_k - x_o). \tag{19}$$

The magnitudes of the potential field vectors expressed in (18) and (19) decrease when they get closer to the obstacle. However, it is desired to increase the potential field when the mobile robot is approaching the obstacle. To modify (17) properly, let us first normalize it as follows:

$$f_{krn} = f_{xkrn}i + f_{ykrn}j = \frac{f_{xkr}}{|f_{kr}|}i + \frac{f_{ykr}}{|f_{kr}|}j \tag{20}$$

where f_{krn} is the normalized form of (17), and then multiply it by $1/r_k^2$ where r_k is related to an ellipse that is tangent to the mobile robot position which is defined as follows:

$$r_k = \sqrt{A^2(x_k - x_o)^2 + B^2(y_k - y_o)^2 - 1}.$$

Therefore, $1/r_k^2$ increases when the mobile robots approach the obstacle, and it enlarges the potential field vector magnitude. On the other hand, the normalized vectors in (20) should be large enough to be able to change the direction of the mobile robot; therefore, the magnitude of these vectors should depend on the magnitude of the desired input force on the mobile robot (without obstacle avoidance) through a function g(.).

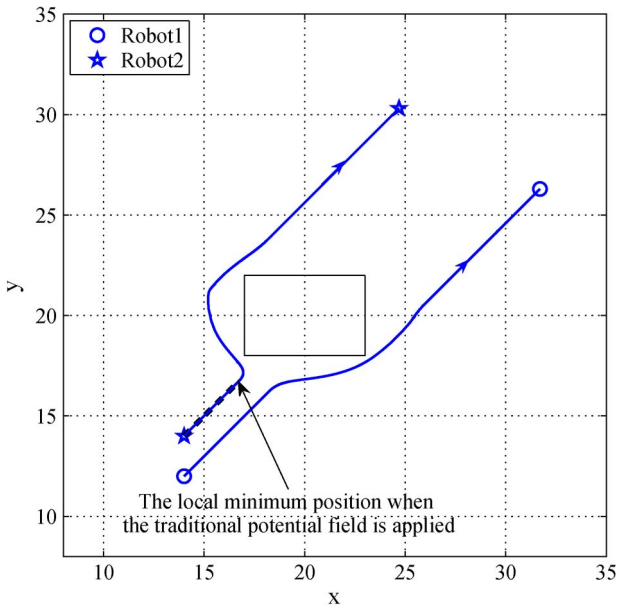

Fig. 4. Obstacle avoidance of two mobile robots in Example 2.

Therefore, the following equations show the input force for obstacle avoidance considering all the aforementioned issues:

$$\textbf{if } r_k \le r_a:$$

$$f_{xk(\mathrm{OA})} = f_{xk\mathrm{des}} + \frac{g\left(|f_{k\mathrm{des}}|\right) f_{xkrn}}{r_k^2}\left(\frac{1}{r_k}-\frac{1}{r_a}\right),$$

$$f_{yk(\mathrm{OA})} = f_{yk\mathrm{des}} + \frac{g\left(|f_{k\mathrm{des}}|\right) f_{ykrn}}{r_k^2}\left(\frac{1}{r_k}-\frac{1}{r_a}\right)$$

$$\textbf{else}:$$

$$f_{xk(\mathrm{OA})} = f_{xk\mathrm{des}}$$

$$f_{yk(\mathrm{OA})} = f_{yk\mathrm{des}} \tag{21}$$

where $f_{k\mathrm{des}} = (f_{xk\mathrm{des}}, f_{yk\mathrm{des}})$ is the desired input force on the mobile robot without obstacle avoidance, $\mathrm{g}(|f_{k\mathrm{des}}|)$ is the function of $f_{k\mathrm{des}}$, and r_a is defined as an ellipse where the potential field vectors are active inside it.

In the last term of (21), $((1/r_k)-(1/r_a))$ helps us to keep the cohesion of the effect of the potential field vectors on the mobile robot. The smaller r_k (closer to the obstacle) yields the larger effect of the potential field for obstacle avoidance.

It should be noted that the target of the mobile robot should not be in the effective region of the obstacle where the potential field is active inside it.

Example 2: Suppose two mobile robots with initial positions (14, 12) and (14, 14) where their input forces are (8, 8), $M=1$, $B=1$, and $k_d=9$. Then, consider $\mathrm{g}(|f_{k\mathrm{des}}|)=|f_{k\mathrm{des}}|$, $r_a=1$, and an obstacle with (20 $\pm$ 3, 20 $\pm$ 2) as its vertices. The trajectories of the two mobile robots are depicted in Fig. 4. The mobile robot shown by $\star$ moves toward the center of the obstacle, and if the traditional potential field is employed, it cancels the input force (8, 8); therefore, the mobile robot sticks in a local minimum position. The trajectory of the mobile robot when the traditional potential field is applied is depicted in Fig. 4 with a dashed line.

As shown in Fig. 4, each mobile robot passes the obstacle based on its direction and relative position to the obstacle. The second terms of $f_{xk(\mathrm{OA})}$ and $f_{yk(\mathrm{OA})}$ in (21) present the effect of the potential field, and based on the definition of the potential field, the resultant of the input forces on the mobile robot will not be zero. In other words, the potential field force cannot cancel the desired input force on the mobile robot. Therefore, the mobile robots do not stick in local minimum positions. This issue is verified in Fig. 3.

The proposed potential field is rotational on ellipses enveloping a rectangular obstacle. It should be noted that, if we can find a method to calculate the equations of ellipses which envelope an obstacle with any shapes (nonrectangular), the proposed approach can be extended for avoiding the obstacle.

B. Behavioral Structure

To extend the proposed approach for obstacle avoidance of swarming mobile robots, the mobile robots should rebuild the formation again, after passing the effective region of the potential field. Therefore, the force which is used for obstacle avoidance should decrease continuously, and the force which is employed for the virtual structure should be increased. Accordingly, to apply the mentioned behavioral structure for obstacle avoidance of a team of swarming mobile robots, (21) for the kth mobile robot should be modified for the conditions that the mobile robot approaches the obstacle and then passes it as follows:

$$\textbf{if } r_k \le r_a:$$

$$f_{xk(\mathrm{BS})} = f_{xk(\mathrm{VS})|_{r_k=r_a}} + \frac{g\left(\left|f_{k(\mathrm{VS})|_{r_k=r_a}}\right|\right) f_{xkrn}}{r_k^2}\left(\frac{1}{r_k}-\frac{1}{r_a}\right),$$

$$f_{yk(\mathrm{BS})} = f_{yk(\mathrm{VS})|_{r_k=r_a}} + \frac{g\left(\left|f_{k(\mathrm{VS})|_{r_k=r_a}}\right|\right) f_{ykrn}}{r_k^2}\left(\frac{1}{r_k}-\frac{1}{r_a}\right) \tag{22}$$

$$\textbf{else (after passing the obstacle)}:$$

$$f_{xk(\mathrm{BS})} = f_{xk(\mathrm{VS})|_{r_k=r_a}}\exp(-\tau r_k) + f_{xk(\mathrm{VS})}\left(1-\exp(-\tau r_k)\right),$$

$$f_{yk(\mathrm{BS})} = f_{yk(\mathrm{VS})|_{r_k=r_a}}\exp(-\tau r_k) + f_{yk(\mathrm{VS})}\left(1-\exp(-\tau r_k)\right) \tag{23}$$

where $f_{k(\mathrm{BS})} = (f_{xk(\mathrm{BS})}, f_{yk(\mathrm{BS})})$ is the input force in the behavioral structure, τ is a positive constant number to have a smooth switching from the strategy for obstacle avoidance to the virtual structure, and the $f_{k(\mathrm{VS})|_{r_k=r_a}} = (f_{xk(\mathrm{VS})|_{r_k=r_a}}, f_{yk(\mathrm{VS})|_{r_k=r_a}})$ is the $f_{k(\mathrm{VS})} = (f_{xk(\mathrm{VS})}, f_{yk(\mathrm{VS})})$ when the formation reaches the obstacle which is considered to keep cohesion in the switching.

To rebuild the formation after passing the obstacle, a feedback from the position of all the mobile robots in the formation is considered to control the position of the virtual mobile robot.

Therefore, the input force on the virtual mobile robot in the behavioral structure can be stated as follows:

$$\textbf{if } r_m \le r_a \ \ (r_m = \text{minimum of } r_k, k \in \{1, 2, \ldots, N\}) :$$

$$f_{xv(\mathrm{BS})} = f_{xv\mathrm{des}} + k_p(x_m - x_v)\left(1 - \exp(-\tau r_m)\right)$$

$$f_{yv(\mathrm{BS})} = f_{yv\mathrm{des}} + k_p(y_m - y_v)\left(1 - \exp(-\tau r_m)\right)$$

$$\textbf{else } (\text{after passing the obstacle}) :$$

$$f_{xv(\mathrm{BS})} = f_{xv\mathrm{des}}$$

$$f_{yv(\mathrm{BS})} = f_{yv\mathrm{des}}$$

where $(f_{xv\mathrm{des}}, f_{yv\mathrm{des}})$ is the desired input force on the virtual mobile robot without obstacle avoidance, k_p is a positive gain of the feedback, and (x_m, y_m) is the mean of the mobile robot positions which can be stated as follows:

$$x_m = \sum_{k=1}^{N} \frac{x_k}{N}, \quad y_m = \sum_{k=1}^{N} \frac{y_k}{N}.$$

V. Simulation Results

The proposed approaches for different formation structures are evaluated by the following scenarios.

Scenario 1: Consider four mobile robots with dynamical equations (7) and the input force given in (9) where their initial positions are (5, 5), (2, 4), (4, 4), and (5, 1). The mobile robots surround a virtual mobile robot with initial position (4, 5). Without loss of generality, consider $M = 1$, $B = 1$, $k_d = 9$, $k_{sk} = 100$, $k \in \{1, 2, 3, 4\}$, $k_r = 10$, $\alpha = 3$, and $q_k = 10$, $k \in \{1, 2, 3, 4\}$. The dynamical equations of the virtual mobile robot are given in (10), where $f_{xv} = 8$ and $f_{yv} = 8\sin((1/4)x_v)$. In practice, the actuators have a limited range of application. To consider this constraint, it is supposed that $|f_k|_{\max} = 20$, $k \in \{1, 2, 3, 4\}$. Fig. 5 shows the four mobile robots around a virtual mobile robot in a square formation for $t = 50$. The figure confirms that the mobile robots reach a square formation with distance $4.24(2 \times 3\sin(\pi/4))$ from their neighbors with negligible errors.

Scenario 2: Now, we repeat the previous scenario when one of the mobile robots fails or exits the formation arbitrarily. Fig. 6 shows that, when the fourth mobile robot exits the formation, the formation changes to a triangle formation automatically. Indeed, when the mobile robots stop and fail to follow the virtual mobile robot, as other mobile robots move and get far from it, forces exerted by the faulty mobile robot will be gradually diminished.

Scenario 3: Now, suppose that there is an obstacle with vertices (25 ± 4, 25 ± 3) and the virtual mobile robot desired input force is (8, 8). Then, consider $\mathrm{g}(|f_{k(\mathrm{VS})|_{r_k=r_a}}|) = |f_{k(\mathrm{VS})|_{r_k=r_a}}|$, $r_a = 1$, $k_p = 10$, and $\tau = 4$. As the mobile robots approach the obstacle, by using (22) and (23), the strategy switches to obstacle avoidance, and after passing the obstacle, the formation of the mobile robot will be rebuilt. Fig. 7 shows this scenario when the formation gets close to the obstacle for $t = 50$.

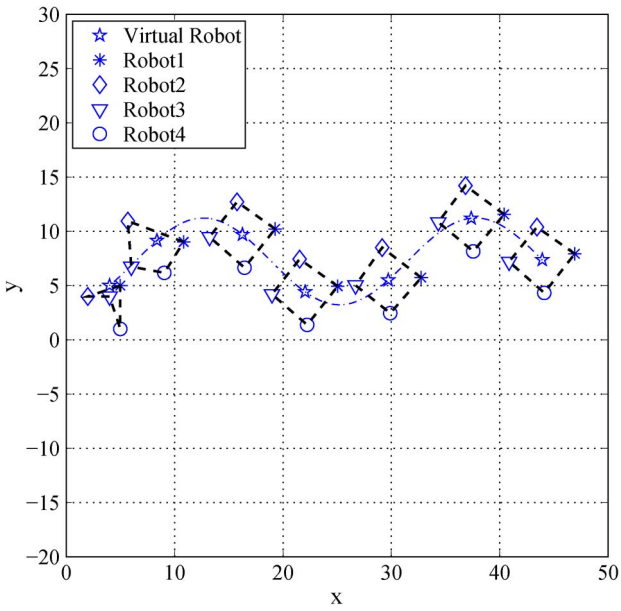

Fig. 5. Mobile robots swarming with square formation in Scenario 1.

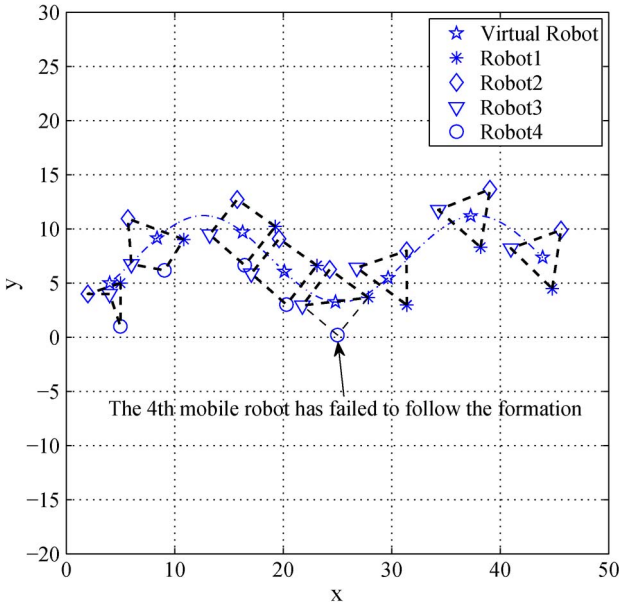

Fig. 6. Swarming of the mobile robots with a square formation in Scenario 2 when one of the mobile robots exits the formation.

VI. Conclusion

In this paper, by using attractive forces toward a circle and by inspiring from the repulsive force between identical electric charges, a control strategy for regular polygon formations of mobile robots was presented based on the virtual structure. In the proposed approach, the distances between the mobile robots regulated autonomously to reach a regular polygon formation, and the formation was maintained while it was moving. It could also be adjusted to the formation changing when some mobile robots exited or entered the formation. A novel method for obstacle avoidance of mobile robots in a formation was also introduced. This method that was based on a rotational potential field prevented the mobile robots to be in contact with

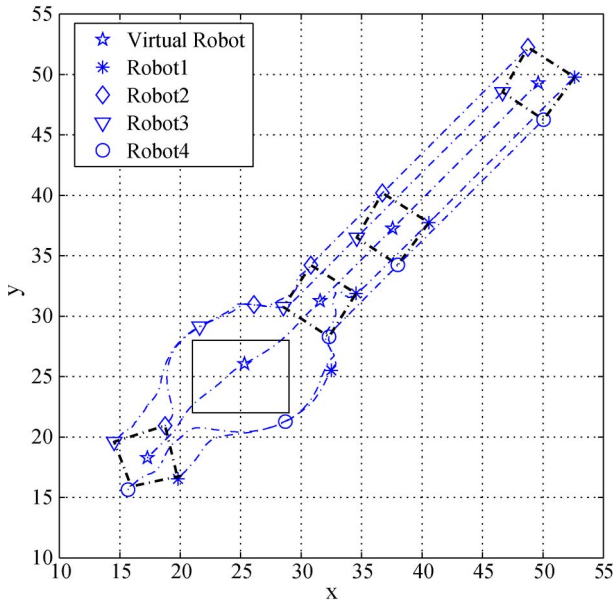

Fig. 7. Obstacle avoidance in Scenario 3 when the formation gets close to an obstacle.

obstacles and led the mobile robots to move toward their desired targets in a smoother trajectory compared to similar techniques in the literature. Although obstacle avoidance approaches used potential fields, the proposed approach prevented vehicles to stick in local minimum positions.

REFERENCES

[1] Z. Wang and D. Gu, "Cooperative target tracking control of multiple robots," *IEEE Trans. Ind. Electron.*, vol. 59, no. 8, pp. 3232–3240, Aug. 2012.
[2] H. Rezaee and F. Abdollahi, "Cross coupled sliding mode controllers for cooperative UAVs with communication delays," in *Proc. 51st IEEE Conf. Decision Control*, Dec. 2012, pp. 3116–3121.
[3] Y. Wang, W. Yan, and W. Yan, "A leader-follower formation control strategy for AUVs based on line-of-sight guidance," in *Proc. IEEE Int. Conf. Mechatron. Autom.*, Aug. 2009, pp. 4863–4867.
[4] J. Ferruz, V. Vega, A. Ollero, and V. Blanco, "Reconfigurable control architecture for distributed systems in the HERO autonomous helicopter," *IEEE Trans. Ind. Electron.*, vol. 58, no. 12, pp. 5311–5318, Dec. 2011.
[5] H. Zhang, F. L. Lewis, and Z. Qu, "Lyapunov, adaptive, and optimal design techniques for cooperative systems on directed communication graphs," *IEEE Trans. Ind. Electron.*, vol. 59, no. 7, pp. 3026–3041, Jul. 2012.
[6] R. W. Beard, J. Lawton, and F. Y. Hadaegh, "A coordination architecture for spacecraft formation control," *IEEE Trans. Control Syst. Technol.*, vol. 9, no. 6, pp. 777–790, Nov. 2001.
[7] H. Rezaee and F. Abdollahi, "Motion synchronization in unmanned aircrafts formation control with communication delays," *Commun. Nonlinear Sci. Numer. Simul.*, vol. 18, no. 3, pp. 744–756, Mar. 2013.
[8] H. Rezaee and F. Abdollahi, "Mobile robots cooperative control and obstacle avoidance using potential field," in *Proc. IEEE/ASME Int. Conf. Adv. Intell. Mechatron.*, Jul. 2011, pp. 61–66.
[9] H. Min, F. Sun, and F. Niu, "Decentralized UAV formation tracking flight control using gyroscopic force," in *Proc. Int. Conf. Comput. Intell. Meas. Syst. Appl.*, Hong Kong, China, May 2009, pp. 91–96.
[10] B. Ranjbar-Sahraei, F. Shabaninia, A. Nemati, and S. D. Stan, "A novel robust decentralized adaptive fuzzy control for swarm formation of multiagent systems," *IEEE Trans. Ind. Electron.*, vol. 59, no. 8, pp. 3124–3134, Aug. 2012.
[11] H. Hashimoto, S. Aso, S. Yokota, A. Sasaki, Y. Ohyama, and H. Kobayashi, "Stability of swarm robot based on local forces of local swarms," in *Proc. SICE Annu. Conf.*, Aug. 2008, pp. 1254–1257.
[12] G. Elkaim and R. Kelbley, "A lightweight formation control methodology for a swarm of non-holonomic vehicles," in *Proc. IEEE Aerosp. Conf.*, Jul. 2006, pp. 1–6.
[13] D. V. Dimarogonas, "Sufficient conditions for decentralized potential functions based controllers using canonical vector fields," *IEEE Trans. Autom. Control*, vol. 57, no. 10, pp. 2621–2626, Oct. 2012.
[14] B. Varghese and G. McKee, "A mathematical model, implementation and study of a swarm system," *Robot. Autonom. Syst.*, vol. 58, no. 3, pp. 287–294, Mar. 2010.
[15] A. Dogan and S. Venkataramanan, "Nonlinear control for reconfiguration of unmanned aerial vehicles formation," *J. Guid., Control, Dyn.*, vol. 28, no. 4, pp. 667–678, Jul./Aug. 2005.
[16] X. Wang, V. Yadav, and S. N. Balakrishnan, "Cooperative UAV formation flying with obstacle/collision avoidance," *IEEE Trans. Control Syst. Technol.*, vol. 15, no. 4, pp. 672–679, Jul. 2007.
[17] D. Zhuoninga, Z. Rulinb, C. Zongji, and Z. Rui, "Study on UAV path planning approach based on fuzzy virtual force," *Chin. J. Aeronaut.*, vol. 23, no. 3, pp. 341–350, Jun. 2010.
[18] H. Cho and S. W. Kim, "Mobile robot localization using biased chirp-spread-spectrum ranging," *IEEE Trans. Ind. Electron.*, vol. 57, no. 8, pp. 2826–2835, Aug. 2010.
[19] L. E. Barnes, M. A. Fields, and K. P. Valavanis, "Swarm formation control utilizing elliptical surfaces and limiting functions," *IEEE Trans. Syst., Man, Cybern. B, Cybern.*, vol. 39, no. 6, pp. 1434–1445, Dec. 2009.
[20] T. Paul, T. R. Krogstad, and J. T. Gravdahl, "UAV formation flight using 3D potential field," in *Proc. 16th Mediterranean Conf. Control Autom.*, Jun. 2008, pp. 1240–1245.
[21] M. Barisic, Z. Vukic, and N. Miskovic, "Effects of rotors on UUV trajectory planning via the virtual potentials method," in *Proc. Mediterranean Conf. Control Autom.*, Jun. 2008, pp. 1144–1149.
[22] H. Rezaee and F. Abdollahi, "Adaptive artificial potential field approach for obstacle avoidance of unmanned aircrafts," in *Proc. IEEE/ASME Int. Conf. Adv. Intell. Mechatron.*, Jul. 2012, pp. 1–6.

Hamed Rezaee (S'10) received the B.Sc. and M.Sc. degrees in control engineering from Amirkabir University of Technology, Tehran, Iran, in 2009 and 2011, respectively, where he is currently working toward the Ph.D. degree in the Department of Electrical Engineering with a research focus on multiagent systems, consensus problems, swarm robotics, and formation flying control.

Farzaneh Abdollahi (S'98–M'09) received the B.Sc. degree in electrical engineering from Isfahan University of Technology, Isfahan, Iran, in 1999, the M.Sc. degree in electrical engineering from Amirkabir University of Technology, Tehran, Iran, in 2003, and the Ph.D. degree in electrical engineering from Concordia University, Montreal, QC, Canada, in 2008.

She is currently an Assistant Professor with Amirkabir University of Technology and a Research Assistant Professor with Concordia University. Her research interests include neural networks, robotics, control of nonlinear systems, control of multiagent networks, and robust and switching control.